Supplementary Information

Dual-targeted Fluorescent Probe for Tracking Polarity and Phase Transition Processes during Lipophagy

Yang Liu,[a] Xiao-Ting Gong,[bd] Kang-Nan Wang,[a*] Simeng He,[c] Yumeng Wang,[a] Qiaowen Lin,[a] Zhiqiang Liu,[a*] Xiaoqiang Yu [a*] and Bin Liu [bd*]

[a]State Key Laboratory of Crystal Materials, Shandong University, Jinan 250100, China.

[b]Department of Chemical and Biomolecular Engineering, National University of Singapore, 4 Engineering Drive 4, Singapore, 117585, Singapore.

[c]Department of Emergency Medicine, Qilu Hospital of Shandong University, Jinan 250012, China.

[d]Joint School of National University of Singapore and Tianjin University, International Campus of Tianjin University, Binhai New City, Fuzhou, 350207, China.

Table of contents

1. Methods

Materials and instruments

All solvents and reagents were sourced commercially and used without further purification. Solvents of either HPLC or spectroscopic grade were used for optical spectroscopic studies. All experiments used ultrapure water. Chemicals and specialized reagents such as 2-(2-bromoethyl)-1,3-dioxolane, 2-methylbenzothiazole, pyrene-1-carbaldehyde, and piperidine were obtained from Bide Pharmatech Ltd., Lyso Tracker™ Green (LTG), Lyso Tracker™ Deep Red (LTDR), Mito Tracker™ Deep Red (MTDR), Nile red, and Lidi Deep Red (LiDR) were procured from Life Technologies. 3-(4, 5-Dimethylthiazol-2-yl)-2, 5-diphenyltetrazolium bromide (MTT), and Oleic acid (OA) was purchased from Sigma Aldrich Co. The lipophagy inhibitor chloroquine (CQ) was purchased from MedChemExpress. The lipophagy inducer verapamil and loperamide were obtained from Sigma Aldrich Co.

^{1}H NMR and ^{13}C NMR spectra were recorded using a Bruker AVANCE 400 spectrometer in either DMSO-d_6 or Chloroform-*d*, with TMS serving as an internal reference. HRMS data were acquired in ESI^{+} mode using an Agilent 6510 Accurate Mass Q-TOF mass spectrometer. UV-Vis absorption spectra of diluted solutions were recorded using a Hitachi U-2910 spectrophotometer. Fluorescence emission spectra were obtained using a Hitachi F-2700 fluorescence spectrometer equipped with a 450 W Xe lamp. The spectral detection concentration of PTZs was uniformly set at 10 μM. The absolute fluorescence quantum yield values for PTZs in Ethyl Acetate (EA), Dimethyl Sulfoxide (DMSO), and

water were determined using a calibrated integrating sphere on C13534-31 (Hamamatsu Photonics). Quantum chemistry calculations were performed using Gaussian 09 software.[1] Ground state geometries were optimized at the B3LYP/6-31G (d, p) level of theory in EA, DMSO, and water. Hydrogen bond (HB) interactions were determined by placing a solvent molecule at the HB-accepting sites in EA, DMSO, and water. The molecular geometries of HB were optimized at the B3LYP-D3/Def2-SVP level in different solvents, and the corresponding interaction energies were calculated at the M062X/Def2-SVP level in solvents.[1] The CIE chromaticity coordinates were determined based on spectral data. MTT assay was performed using a Tecan Infinite M200 Pro microplate reader. Images of the probes were captured using an Olympus FV1200 confocal laser scanning microscope.

Single crystal X-ray diffraction

The crystals of PTZ were obtained by allowing the solvent (dichloromethane and ethanol) to evaporate slowly. Single crystal X-Ray diffraction data were collected using a Rigaku RAXIS-PRID diffractometer in ω-scan mode using graphite-monochromated Cu-Kα radiation, and the crystal structure of PTZ was determined using the SHELXTL program and refined with full-matrix least squares on F^2. Anisotropic refinement was performed for nonhydrogen atoms, while the positions of hydrogen atoms were calculated and refined isotropically. [CCDC No. 2270087 for PTZ contains the supplementary crystallographic data for this paper].

Monitoring solvent phase transitions

The images and video of the dynamic changes of the probes in different liquid phases were captured by an iPhone under 365 nm UV lamps. Probe stock solutions (2 mM) were prepared in DMSO.

The group of EA, DMSO and water: Firstly, 2 mL of EA solvent was added to a four-sided transmitting cuvette. Then a 10 μL of the probe stock solution was added to 2 mL of EA solution to obtain a working solution. Subsequently, 0.2 mL of pure water was added to this working solution. Next, 0.8 mL of DMSO was gradually added in an equal gradient. In this state, DMSO was mixed with water and EA. The upper and lower two-phase solutions in the static state exhibited blue and orange fluorescence, respectively, indicating phase separation. Continuous injection of 0.5 mL of DMSO disrupted the equilibrium of the two phases, resulting in complete fusion of the three phases and the display of orange fluorescence. The reverse titration of EA, DMSO, and water was performed in the reverse order of adding solvents as described above.

The group of TOL (Toluene), MeOH (Methanol) and water: Firstly, 1.5 mL of TOL solvent was added to cuvette. Then, a 10 μL of probe stock solution was added to TOL working solution. Subsequently, 0.2 mL of pure water was added to this working solution. Next, 1 mL of DMSO was gradually added in an equal gradient. In this state, DMSO was mixed with water and MeOH. Continuous injection of 0.8 mL of DMSO resulted in the complete fusion of the three phases and the display of orange fluorescence.

Cell culture and cytotoxicity

HeLa cells were obtained from the Experimental Animal Centre of Shandong University. The cells were cultured in DMEM medium supplemented with 10% FBS (Gibco BRL), 100 μg/mL streptomycin (Gibco BRL), and 100 U/mL penicillin (Gibco BRL). The cell culture was maintained in a humidified incubator at 37 °C and 5% CO_2.

To assess the cytotoxicity of PTZs, HeLa cells in the logarithmic growth phase were seeded into 96-well plates and allowed to adhere for 1 h or 24 h. Various concentrations of the probes (0, 3.125, 6.25, 12.5, 25, 50, and 100 μM) were added to the wells, and the cells were treated for 24 h. Then 20 μL of MTT reagent (5 mg/mL) was added to each well and incubated for 4 h. The purple crystals formed were dissolved in DMSO (100 μL), and the absorbance was measured at 570 nm for 20 min using a microplate reader. Moreover, cytotoxicity experiments were repeated three times.

Cell imaging

Co-localization imaging and photostability experiments for PTZ: HeLa cells were seeded in 35 mm culture dishes and incubated for 24 h. After incubation with PTZ (500 nM) at 37 °C for 2 min, LTDR (200 nM) or LiDR (200 nM) was added. After another 10 min of incubation, the cells were visualized using confocal microscopy without washing. The excitation and emission ranges of the dyes in confocal imaging were as follows: λ_{ex} = 405 nm, λ_{em1} = 430-480 nm, λ_{em2} = 570-630 nm for PTZ; λ_{ex} = 633 nm, λ_{em} = 640-700 nm for

LTDR; λ_{ex} = 633 nm, λ_{em} = 645-705 nm for LiDR; λ_{ex} = 543 nm, λ_{em} = 600-660 nm for Nile red; λ_{ex} = 488 nm, λ_{em} = 500-560 nm for LTG.

Co-localization experiments for PTZ-OH and PTZ-Me: HeLa cells were seeded in 35 mm culture dishes and incubated for 24 h. After incubation with PTZ-OH or PTZ-Me (1 μM) at 37 °C for 10 min, LTDR (200 nM) or LiDR (200 nM) was added. After another 10 min of incubation, the cells were visualized using confocal microscopy without washing. The excitation and emission range of the dyes in confocal imaging were as follows: λ_{ex} = 405 nm, λ_{em1} = 430-480 nm, λ_{em2} = 570-630 nm for PTZ-OH and PTZ-Me;

Signal-to-noise ratio experiments: Signal-to-noise ratio experiments were carried out on Olympus FV1200 confocal laser scanning microscope. HeLa cells were stained with PTZ and commercial probes (Nile red, LiDR, LTG, and LTDR), respectively, under the same concentration (10 μM). Subsequently, the fluorescence intensity ratio of the fluorescent region stained by the probe to the adjacent background region was calculated using Image J software.

Dynamic tracking of lipid droplets and lysosomes: For dynamic tracking lipid droplets and lysosomes in living cells, the different experimental group was incubated with 800 nM of probes after incubation in DMEM for 15 min at 37 °C, then directly used for imaging. The organelle number and size in live cells was calculated by Image J software.

Dynamic lipophagy process tracking: The living cells treated with EBSS promote the process of lipophagy. Then the cells were used for imaging. Microscopic images of the cells were obtained without wash-out steps.

Spectral measurement

Spectral measurements in different solvents: The probe stock solutions (2 mM) were prepared in DMSO. Then, the UV-vis absorption and fluorescence spectra (excitation wavelength: 405 nm and 488 nm) of probes were measured in different solvents (EA, acetone, tetrahydrofuran, methanol, DMSO, and water) at a work concentration of 10 μM.

Solvent dielectric constant response measurements: Various volume ratios of EA and DMSO mixtures (0% to 10% by volume of DMSO) were prepared to measure the UV-vis absorption and fluorescence spectra of the probes in solvent mixtures of different polarities.

The pH and viscosity response experiments: For viscosity response experiments, the emission spectra were measured in different percentage of glycerin (Gly) and methanol solution (v/v). For pH response experiments, the emission spectra were measured in different pH buffer solutions (NaH_2PO_4-Na_2HPO_4).

Statistical analysis

All the quantitative data were described using the mean SD (standard deviations). Statistical analysis was performed with Student's *t*-test and one-way ANOVA via GraphPad Prism 8.0. $p<0.05$was considered statistically significant (*$p < 0.05$).

Western blot measurements

HeLa cells were cultured in 6-well plates at a density of 1×10^6 cells per well. After incubation, 100 μL of cell lysates were collected to extract the proteins. The protein concentrations were determined using a BCA commercial kit (Beyotime, P0012S). Subsequently, the protein samples were subjected to electrophoresis on 12% SDS-PAGE gels at 80 V for 60 min and then at 120 V for 30 min. Using a transfer apparatus, the separated proteins were transferred onto PVDF membranes (Millipore, 0.22 μm). After blocking with a TBST solution containing 5% skimmed milk for 1-2 h, the membranes were incubated overnight at 4 °C with primary antibodies, including anti-LC3B (1:2000, Abcam, ab192890), anti-SQSTM1/p62 (1:2000, Abcam, ab91526), and anti-GAPDH antibody (1:50000, Proteintech, 60004-1-Ig). After washing the membranes five times with TBST, appropriate secondary antibodies HRP-goat anti-mouse IgG at 1:10000, Proteintech, SA00001-1, and HRP-goat anti-rabbit IgG at 1:10000, Proteintech, SA00001-2 were incubated with the membranes. Finally, the protein bands were detected using chemiluminescence methods, and the gray values were analyzed using Image J software (version 1.8.0).

2. Synthesis and characterization

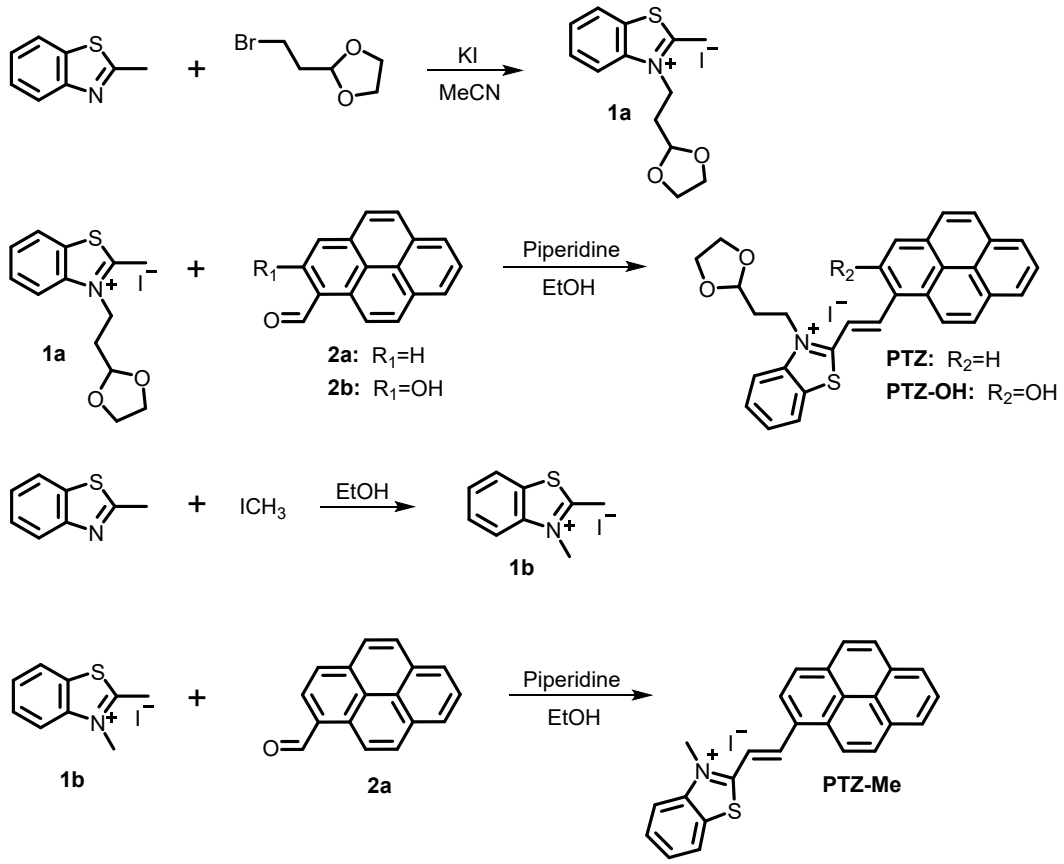

Scheme S1 The synthesis routes of probe PTZ, PTZ-OH, and PTZ-Me.

3-(2-(1, 3-Dioxolan-2-yl)ethyl)-2-methylbenzo[d]thiazol-3-ium (compound 1a). KI (2.00 g, 12 mmol) and 2-(2-bromoethyl)-1,3-dioxolane (1.80 g, 10 mmol) were heated in acetonitrile (50 mL) at 60 °C for 1 h under an oil bath. 2-Methylbenzothiazole (1.49 g, 10 mmol) was added to the above solution and refluxed for 48 h.[2] The solution was cooled to room temperature, 250 mL of ethyl ether solution was added. Then the precipitate was filtered off and collected. After cooling to room temperature, the solution was washed three times with ethyl ether (3 × 15 mL). After solvent removal compound 1a was obtained after drying in air as a dark-brown solid (1.09 g, 28% yield). ^{1}H NMR (400 MHz, DMSO-d_6) δ 8.49 (dd, J = 8.1, 1.2 Hz, 1H), 8.29 (d, J = 8.4 Hz, 1H), 7.96 - 7.87 (m, 1H), 7.81 (t, J =

7.7 Hz, 1H), 5.02 (t, J = 4.3 Hz, 1H), 4.82 (t, J = 7.1 Hz, 3H), 3.94 - 3.70 (m, 4H), 3.24 (s, 3H), 2.28 (td, J = 7.1, 4.3 Hz, 2H).

2, 3-Dimethylbenzo[d]thiazol-3-ium (compound 1b). 2-Methylbenzothiazole (1.49 g, 10 mmol) and iodomethane (1.41 g, 10 mmol) were heated reflux in ethanol (50 mL) for 24 h under oil bath. The solution was cooled to room temperature to produce a precipitate. The precipitate was collected and washed three times with ethanol (3 × 15 mL). Then the solvent is removed to obtained compound 1b as a brown solid (1.95 g, 67% yield). ^{1}H NMR (400 MHz, DMSO-d_6) δ 8.47 (dd, J = 8.2, 1.2 Hz, 1H), 8.36 - 8.24 (m, 1H), 7.89 (m, J = 8.5, 7.3, 1.3 Hz, 1H), 7.80 (m, J = 8.2, 7.2, 1.1 Hz, 1H), 4.22 (s, 3H), 3.20 (s, 3H).

(E)-3-(2-(1,3-Dioxolan-2-yl)ethyl)-2-(2-(pyren-1-yl)vinyl)benzo[d]thiazol-3-ium (PTZ). A solution of the mixture of compound 1a (0.45 g, 1.2 mmol), pyrene-1-carbaldehyde (compound 2a, 0.23 g, 1 mmol), and piperidine (0.1 mL) in absolute ethanol (20 mL) was heated reflux (oil bath) for 12 h. The solution is cooled to room temperature until a solid is precipitated and crude product was obtained by filtration. The crude product was recrystallized by dissolving in hot absolute ethanol (15 mL). The hot solution was cooled to room temperature until solid was precipitated.[3] Then the solid was washed with boiling methylbenzene (3 × 15 mL) to obtain pure compound PTZ as a dark red solid (0.34 g, 58% yield). ^{1}H NMR (400 MHz, Chloroform-d) δ 9.17 (dd, J = 8.4, 5.5 Hz, 1H), 8.95 (dd, J = 15.4, 5.4 Hz, 1H), 8.78 (d, J = 9.4 Hz, 1H), 8.32 (dd, J = 12.3, 3.0 Hz, 2H), 8.24 - 8.13 (m, 3H), 8.09 - 7.90 (m, 4H), 7.37 (s, 1H), 7.18 - 7.10 (m, 2H), 5.01 (t, J = 6.7 Hz, 2H), 4.76 (t, J = 4.4 Hz, 1H), 3.56 (dq, J = 9.2, 7.0 Hz, 2H), 3.41 (dq, J = 9.2, 7.0 Hz, 2H),

2.19 (q, J = 6.5 Hz, 2H). ^{13}C NMR (101 MHz, DMSO-d_6) δ 173.46, 158.00, 142.34, 141.72, 135.73, 132.54, 131.09, 130.36, 130.12, 129.97, 129.53, 128.69, 128.46, 127.64, 127.38, 127.04, 126.27, 124.79, 124.13, 122.97, 119.28, 117.39, 117.09, 115.46, 112.73, 101.42, 64.93, 61.92, 55.42, 31.73, 29.51, 29.30, 29.18, 29.05, 27.02, 25.59, 22.57, 15.48, 14.44. HRMS: calculated for $C_{30}H_{24}NO_2S$ [M - I]$^+$: 462.1523 (m/z), found 462.1667.

(E)-3-(2-(1,3-Dioxolan-2-yl)ethyl)-2-(2-(2-hydroxypyren-1-yl)vinyl)benzo[d]thiazol-3-ium (PTZ-OH). A solution of the mixture of 2-hydroxypyrene-1-carbaldehyde (compound 2b, 0.25 g, 1 mmol), compound 1a (0.45 g, 1.2 mmol) and piperidine (0.1 mL) in absolute ethanol (20 mL) was heated for 12 h. After cooling to room temperature, the mixture was filtered, and the precipitation was washed with boiling methylbenzene (3 × 15 mL) to get the product PTZ-OH (dark red solid; 0.27 g, 45% yield). ^{1}H NMR (400 MHz, DMSO-d_6) δ 11.81 (s, 1H), 8.98 (d, J = 15.5 Hz, 1H), 8.74 (d, J = 9.5 Hz, 1H), 8.57 - 8.22 (m, 7H), 8.11 - 8.01 (m, 2H), 7.95 - 7.78 (m, 3H), 5.04 (t, J = 4.0 Hz, 1H), 4.93 (t, J = 6.9 Hz, 2H), 3.92 - 3.83 (m, 2H), 3.83 - 3.73 (m, 2H), 2.37 (td, J = 6.9, 4.1 Hz, 2H). ^{13}C NMR (101 MHz, DMSO-d_6) δ 172.13, 144.64, 141.87, 134.26, 131.27, 130.79, 130.62, 130.44, 130.03, 128.94, 128.71, 127.94, 127.92, 127.52, 127.25, 126.10, 125.97, 124.86, 124.50, 123.97, 123.21, 117.46, 116.18, 100.67, 61.93, 32.72, 15.48. HRMS: calculated for $C_{30}H_{24}NO_3S$ [M - I]$^+$: 478.1472 (m/z), found 478.1528.

(E)-3-Methyl-2-(2-(pyren-1-yl)vinyl)benzo[d]thiazol-3-ium (PTZ-Me). A solution of the mixture of compound 2a (0.23 g, 1 mmol), compound 1b (0.35 g, 1.2 mmol) and piperidine (0.1 mL) in absolute ethanol (20 mL) was heated for 12 h. After cooling to room

temperature, the mixture was filtered, and the precipitation was washed with boiling methylbenzene (3 × 15 mL) to get the product PTZ-Me (shiny red solid; 0.34 g, 67% yield). ^{1}H NMR (400 MHz, DMSO-d_6) δ 9.20 (d, J = 15.5 Hz, 1H), 8.98 (d, J = 8.4 Hz, 1H), 8.90 (d, J = 9.5 Hz, 1H), 8.56 - 8.42 (m, 5H), 8.41 - 8.25 (m, 4H), 8.19 (t, J = 7.6 Hz, 1H), 7.88 (m, 2H), 4.46 (s, 3H). ^{13}C NMR (101 MHz, DMSO-d_6) δ 171.98, 144.62, 142.54, 134.25, 131.27, 130.80, 130.61, 130.42, 130.02, 129.00, 128.59, 127.91, 127.85, 127.50, 127.22, 126.21, 125.99, 124.69, 124.51, 123.99, 123.17, 117.42, 115.95, 39.89, 36.98. HRMS: calculated for $C_{26}H_{18}NS$ $[M - I]^+$: 376.1155 (m/z), found 376.1167.

3. Structural characterizations

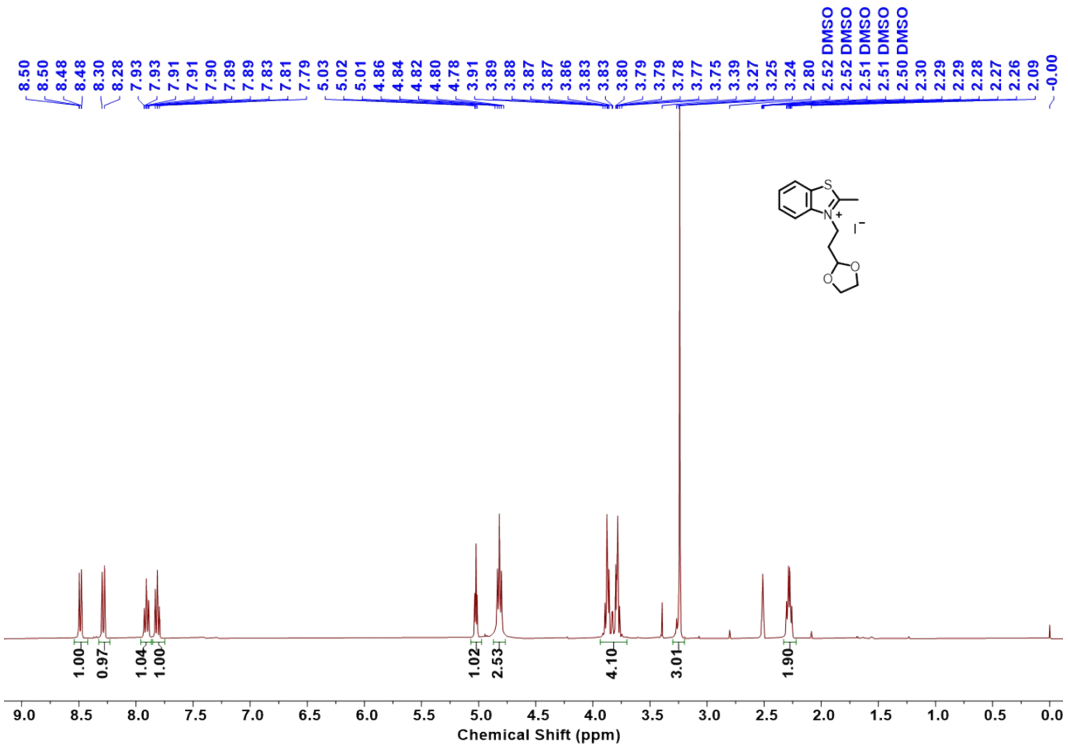

Fig. S1 ^{1}H NMR spectrum of compound 1a in DMSO-d_6.

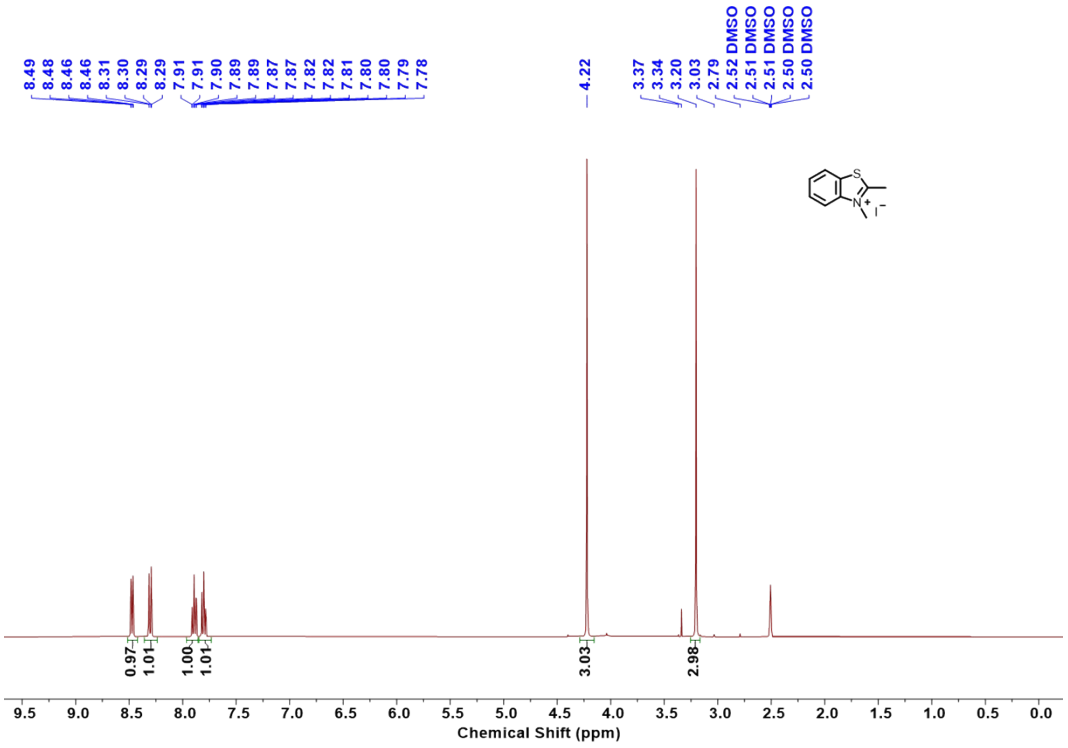

Fig. S2 ^{1}H NMR spectrum of compound 1b in DMSO-d_6.

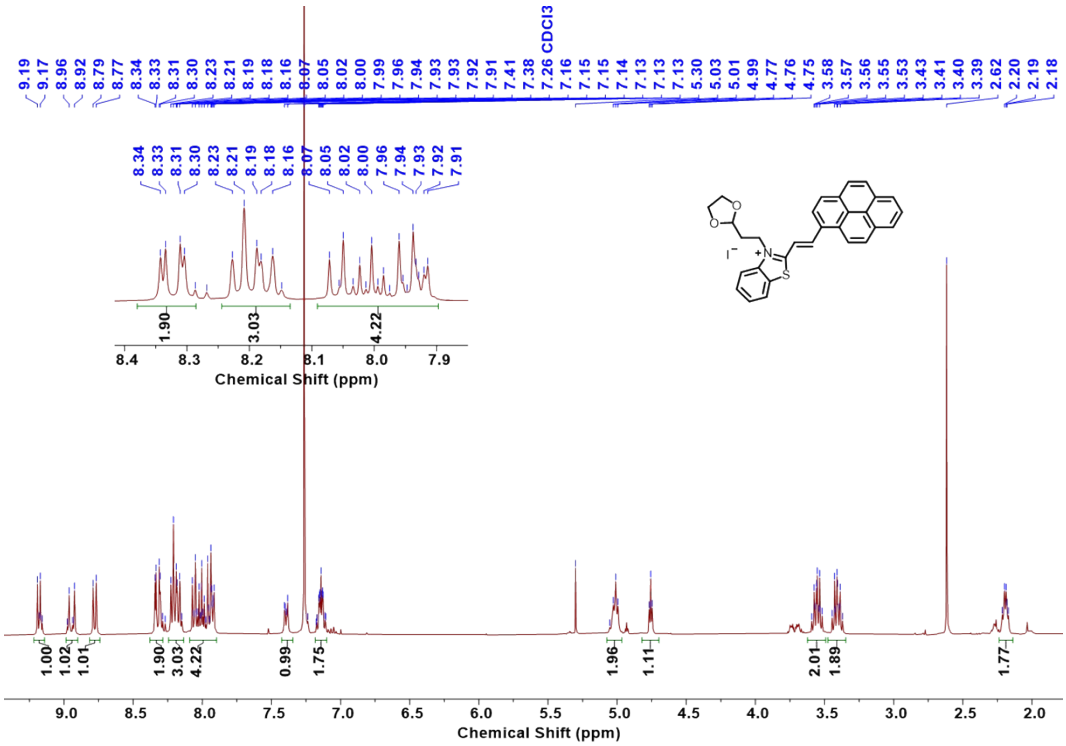

Fig. S3 ^{1}H NMR spectrum of PTZ in Chloroform-*d*.

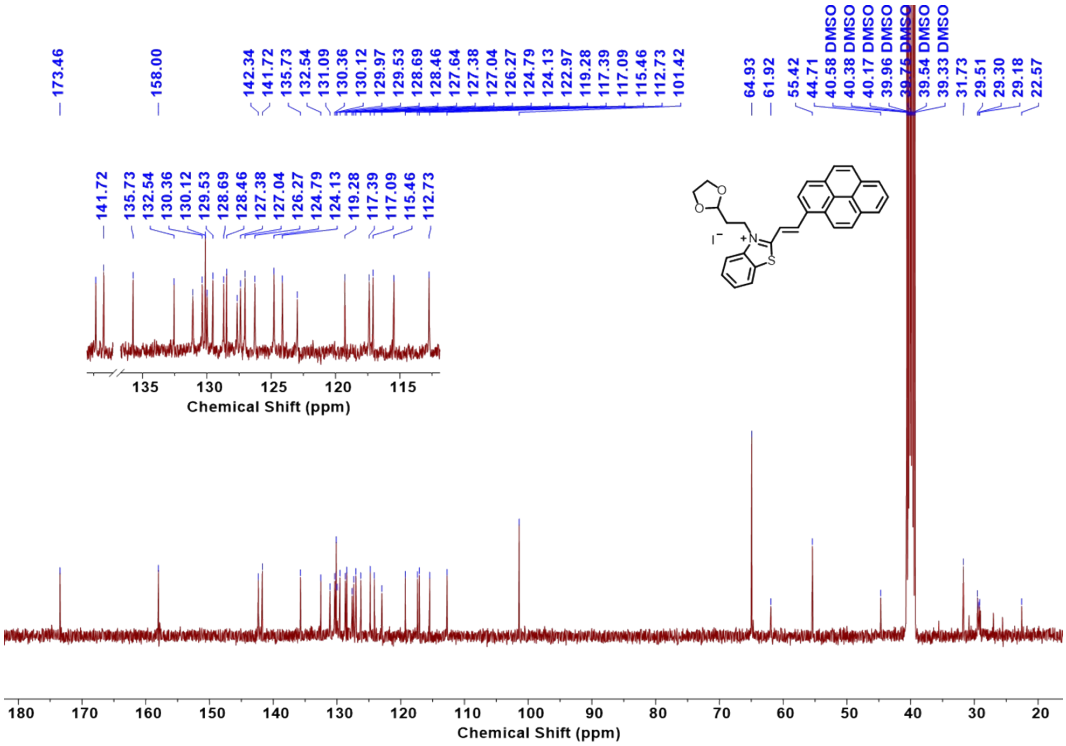

Fig. S4 ^{13}C NMR spectrum of PTZ in DMSO-d_6.

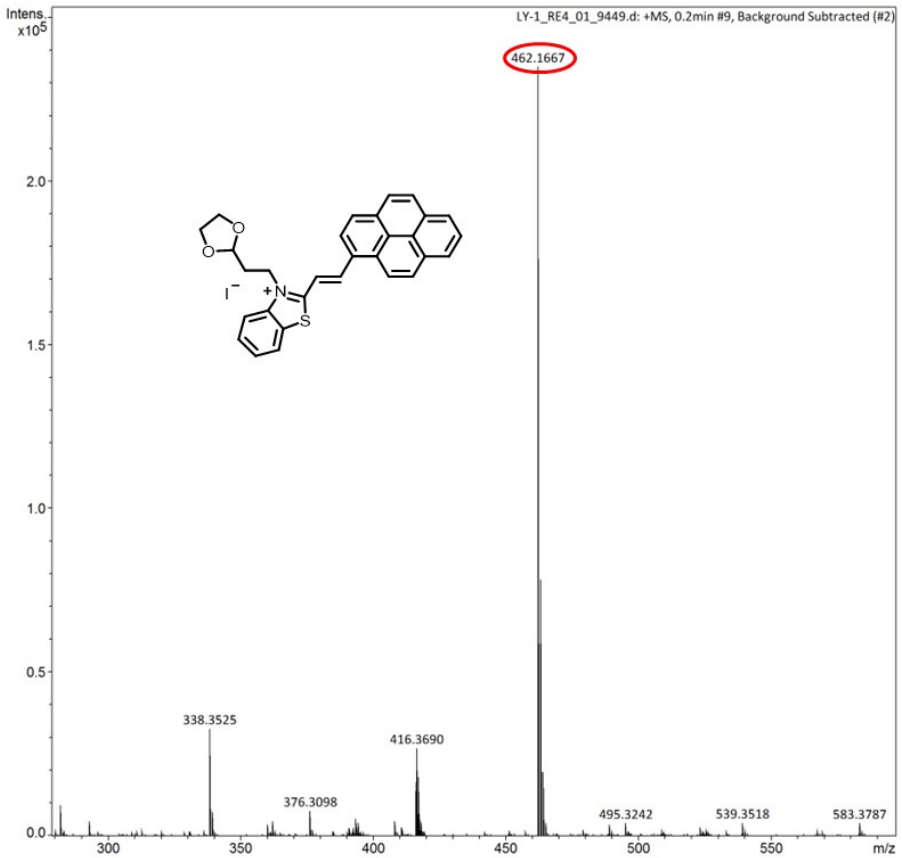

Fig. S5 HRMS spectrum of PTZ.

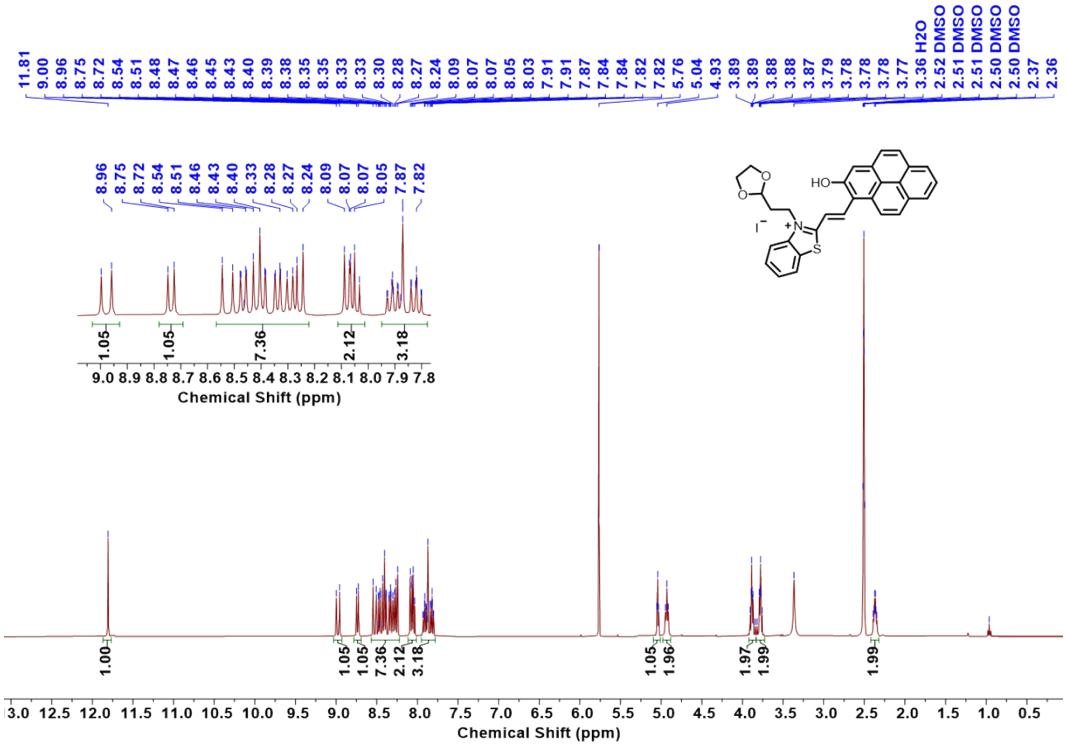

Fig. S6 ^{1}H NMR spectrum of PTZ-OH in DMSO-d_6.

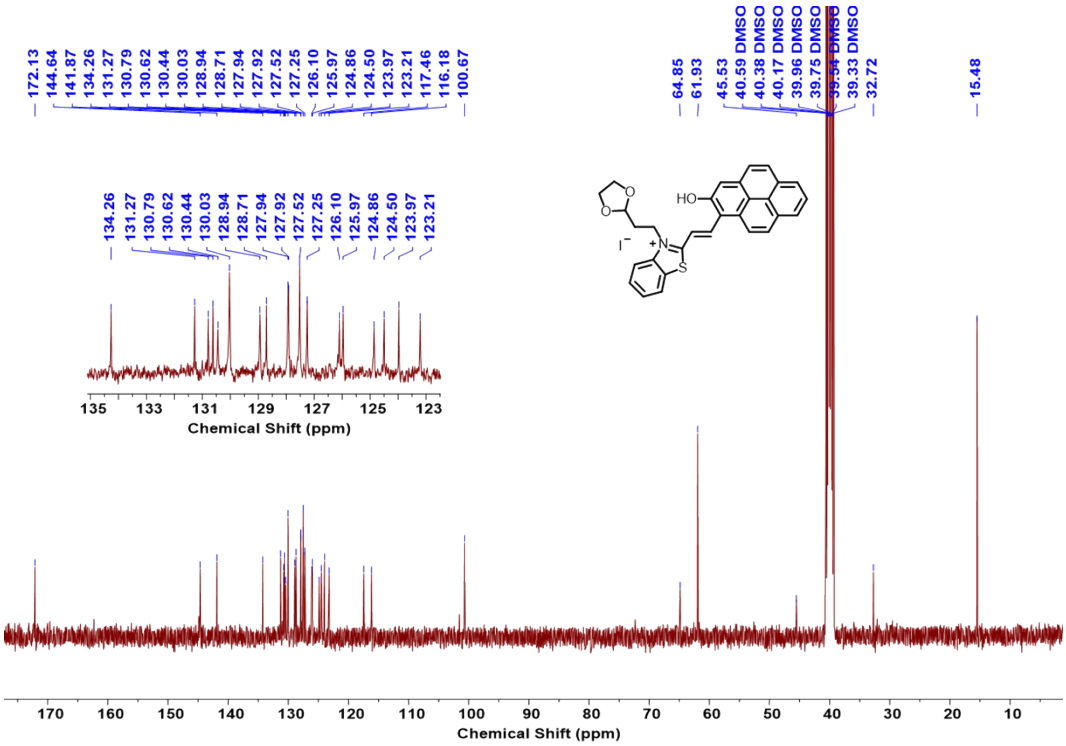

Fig. S7 ^{13}C NMR spectrum of PTZ-OH in DMSO-d_6.

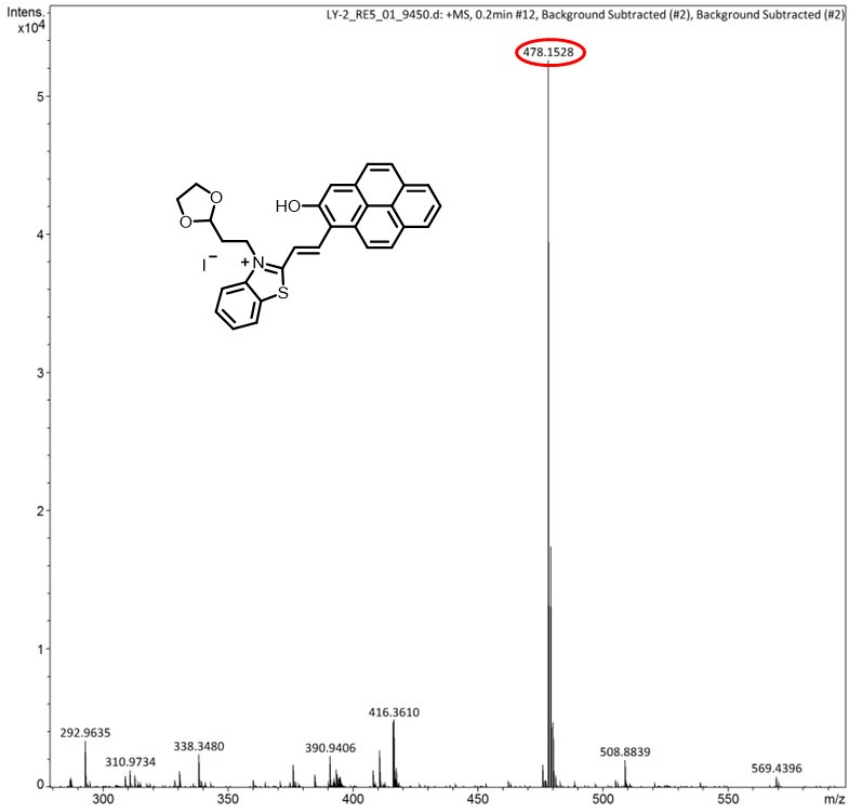

Fig. S8 HRMS spectrum of PTZ-OH.

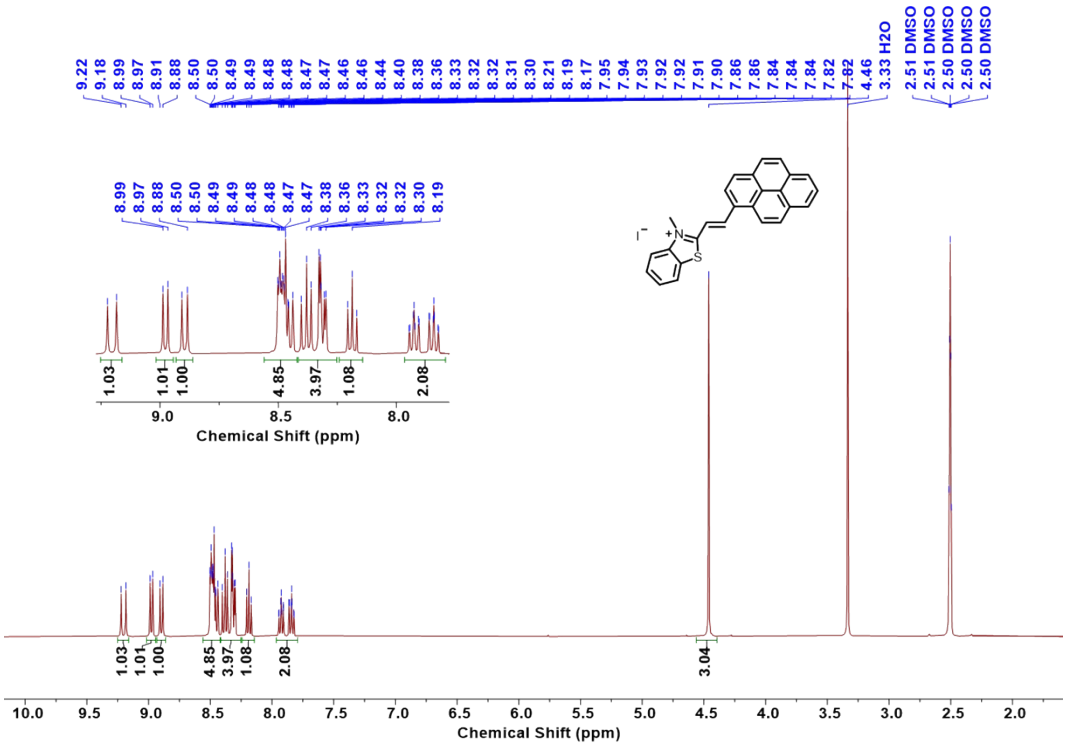

Fig. S9 ^{1}H NMR spectrum of PTZ-Me in DMSO-d_6.

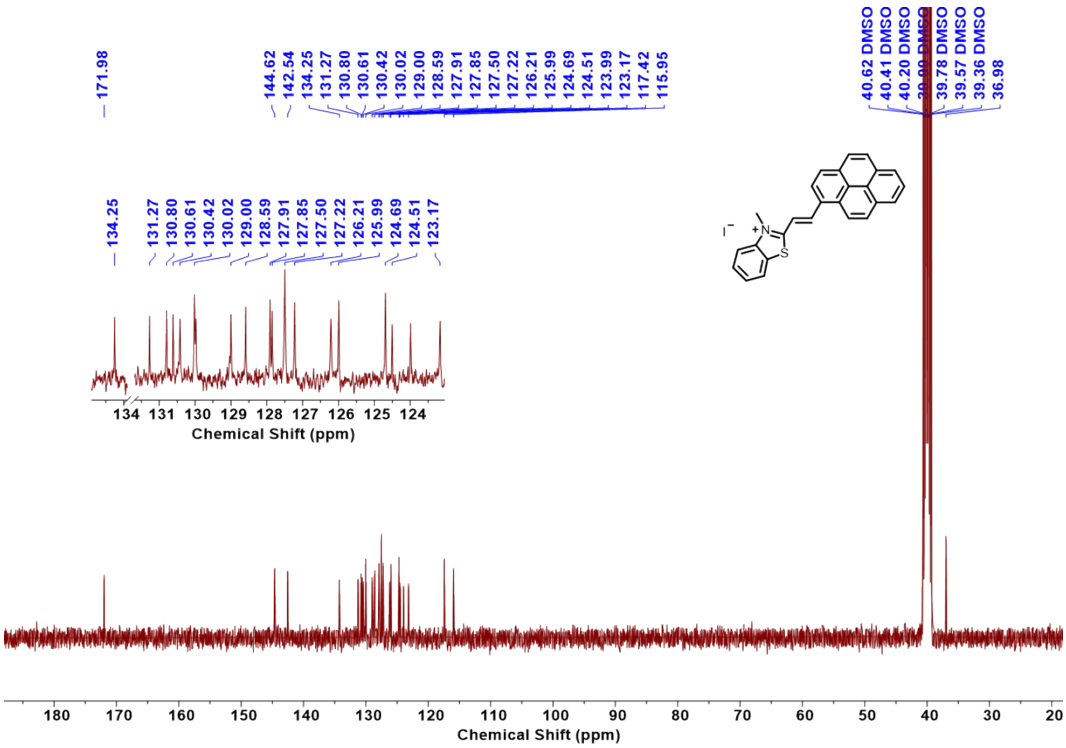

Fig. S10 ^{13}C NMR spectrum of PTZ-Me in DMSO-d_6.

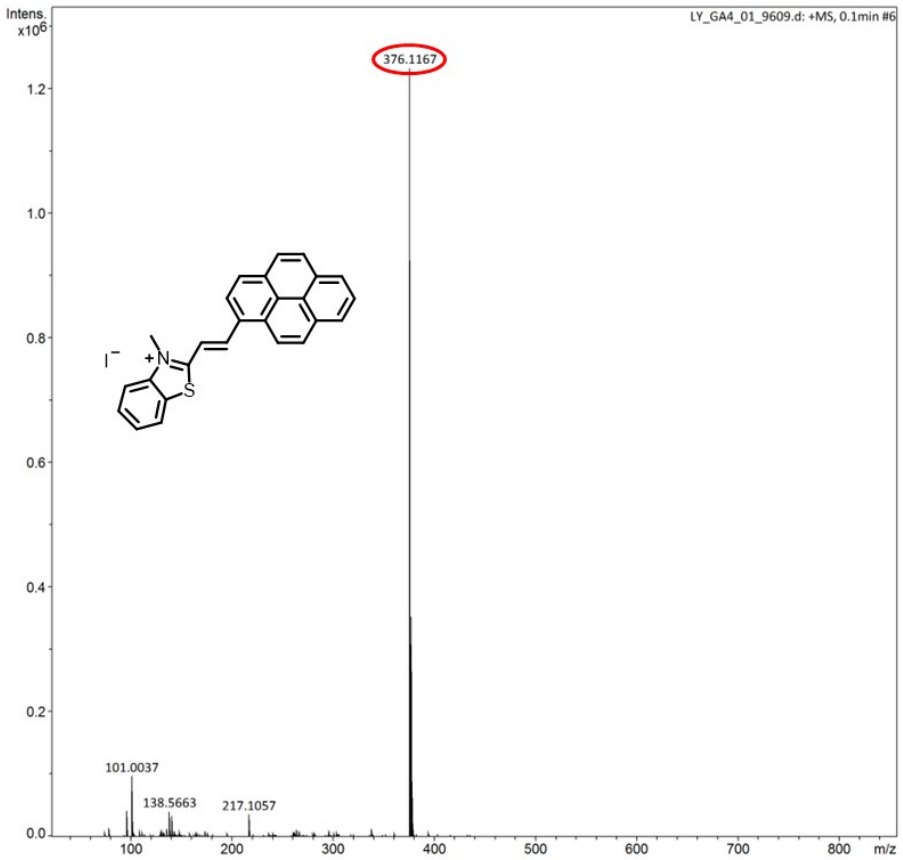

Fig. S11 HRMS spectrum of PTZ-Me.

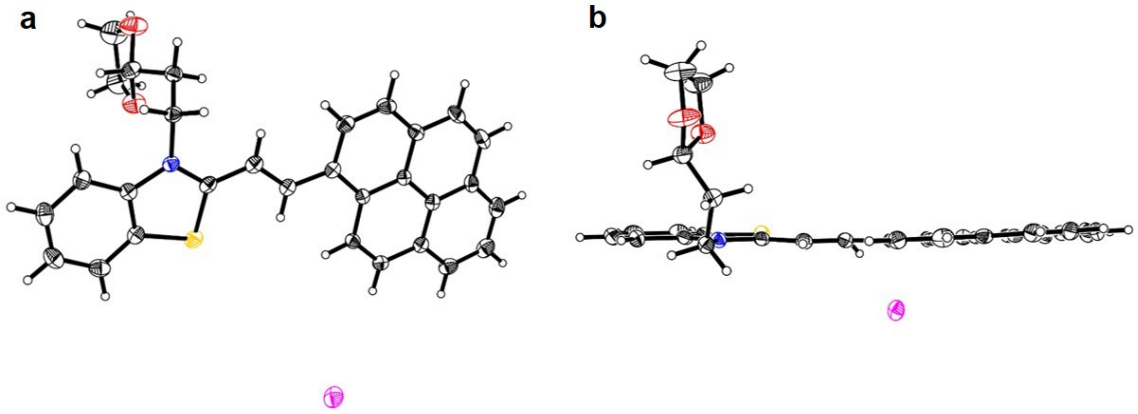

Fig. S12 Single crystal structure of PTZ, top view (**a**) and side view (**b**). Atom color: carbon (lightgray), nitrogen (blue), oxygen (red), sulgur (yellow), lodine (magenta). Displacement ellipsoids displayed at 50% probability level.

4. Optical measurements and cell experiments

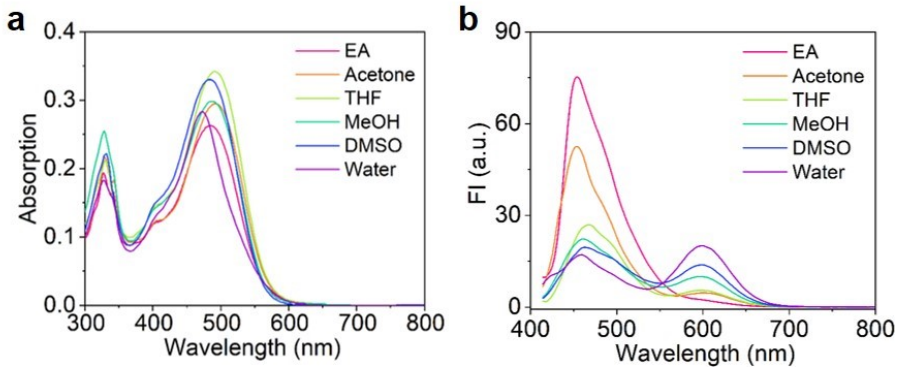

Fig. S13 Absorption (**a**) and fluorescence (**b**) spectra in different solvent of PTZ. λ_{ex} = 405 nm.

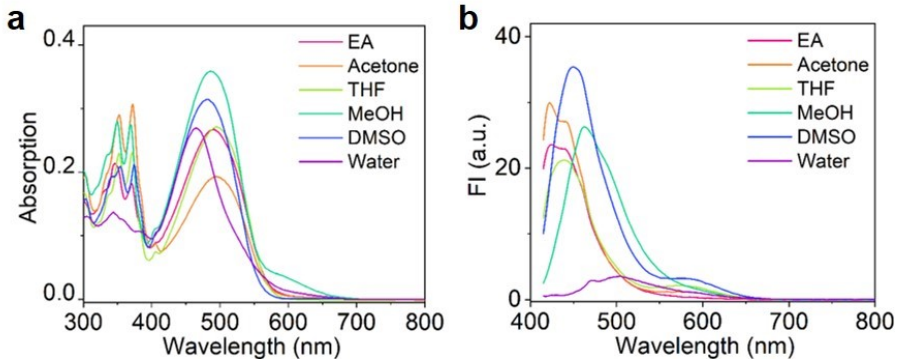

Fig. S14 Absorption (**a**) and fluorescence (**b**) spectra in different solvent of PTZ-OH. λ_{ex} = 405 nm.

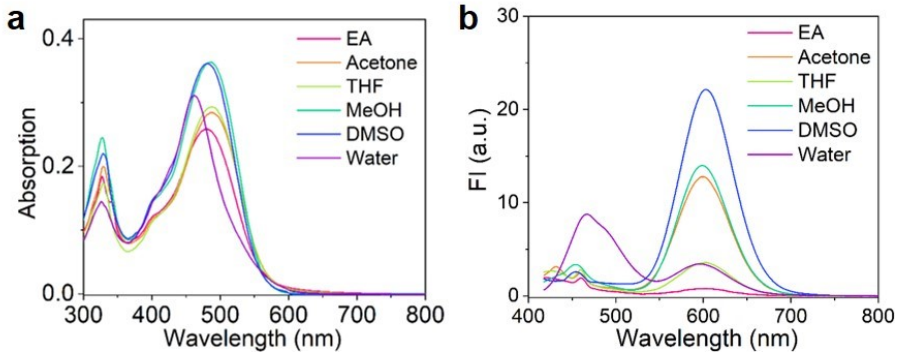

Fig. S15 Absorption (**a**) and fluorescence (**b**) spectra in different solvent of PTZ-Me. λ_{ex} = 405 nm.

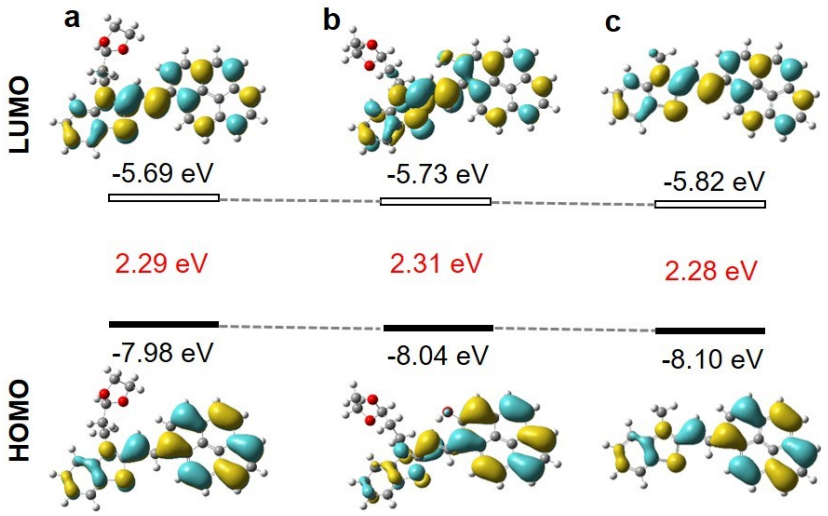

Fig. S16 The spatial electron distributions of HOMO and LUMO of PTZ (**a**), PTZ-OH (**b**), and PTZ-Me (**c**) at the B3LYP/6-31G (d, p) level.

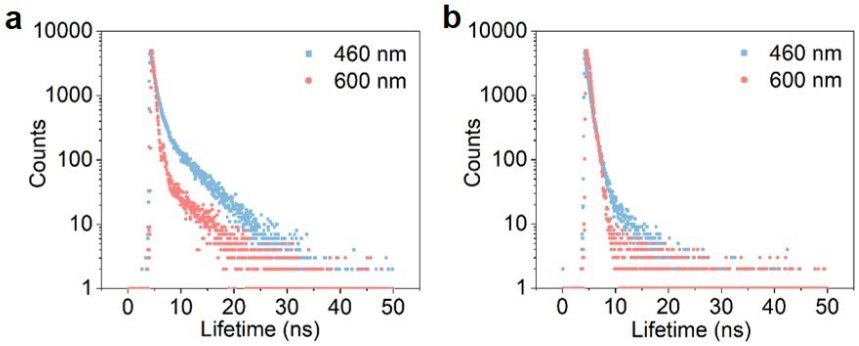

Fig. S17 Fluorescence lifetimes of probe PTZ in EA (**a**) and DMSO (**b**) excited under 460 nm and 600 nm, respectively.

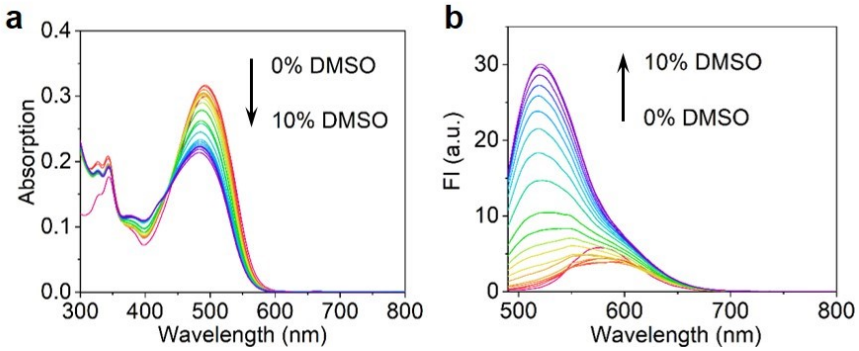

Fig. S18 Absorption (**a**) and fluorescence (**b**) spectra of PTZ-OH in EA/DMSO mixtures with different DMSO fractions (0%-10%), λ_{ex} = 488 nm.

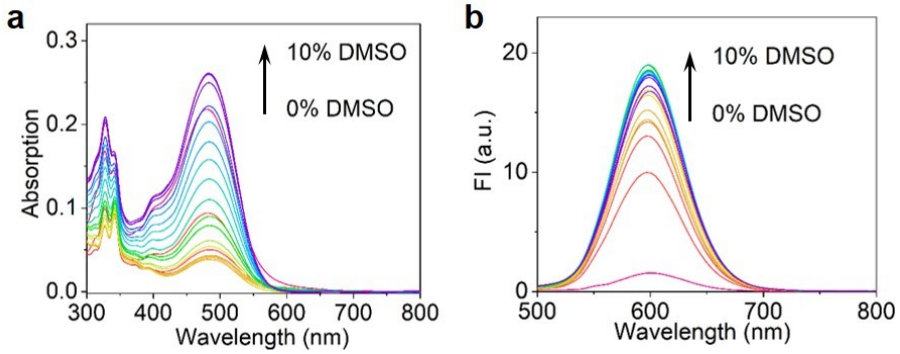

Fig. S19 Absorption (**a**) and fluorescence (**b**) spectra of PTZ-Me in EA/DMSO mixtures with different DMSO fractions (0%-10%), λ_{ex} = 488 nm.

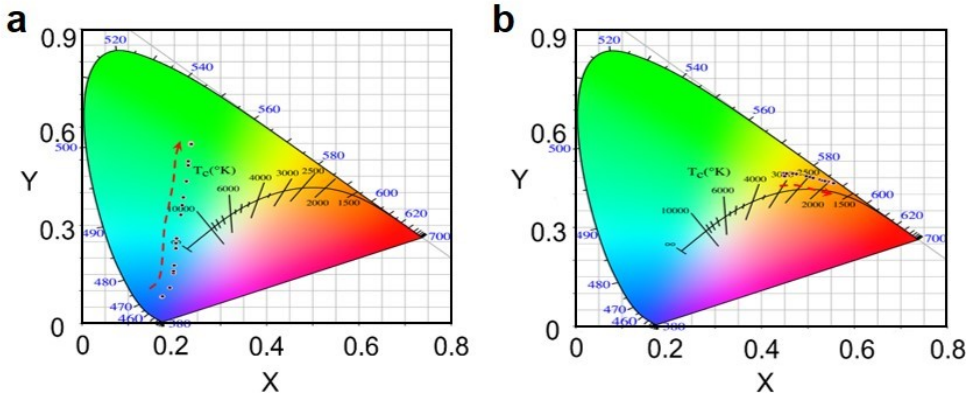

Fig. S20 CIE1931 coordinates of PTZ-OH (**a**) and PTZ-Me (**b**) in EA/DMSO mixtures with different DMSO fractions (0%-10%).

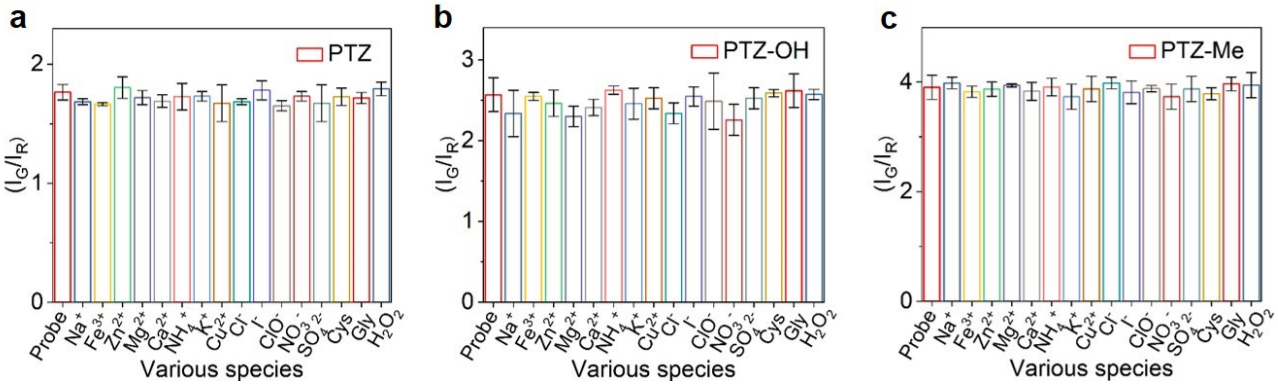

Fig. S21 The fluorescence intensity ratio (I_G/I_R) of PTZ (**a**), PTZ-OH (**b**), and PTZ-Me (**c**) (10 μM) in ultrapure water in the presence of 100 μM different analytes, λ_{ex} = 405 nm. I_G/I_R: The fluorescence intensity ratio of short- and long-wavelength emission.

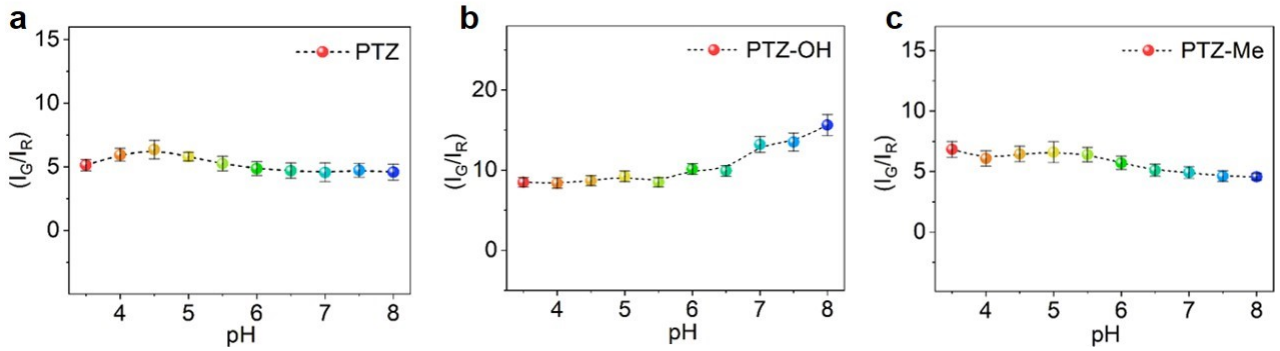

Fig. S22 The fluorescence intensity ratio (I_G/I_R) of PTZ (**a**), PTZ-OH (**b**), and PTZ-Me (**c**) (10 μM) in buffer solution with different physiological pH at room temperature, λ_{ex} = 405 nm. I_G/I_R: The fluorescence intensity ratio of short- and long-wavelength emission.

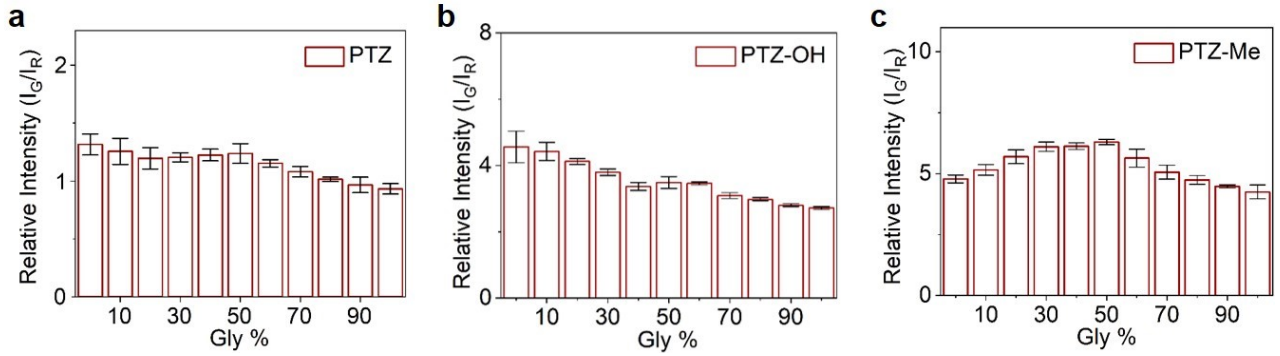

Fig. S23 The fluorescence intensity ratio (I_G/I_R) of PTZ (**a**), PTZ-OH (**b**), and PTZ-Me (**c**) (10 μM) in MeOH/Gly mixtures, λ_{ex} = 405 nm. I_G/I_R: The fluorescence intensity ratio of short- and long-wavelength emission.

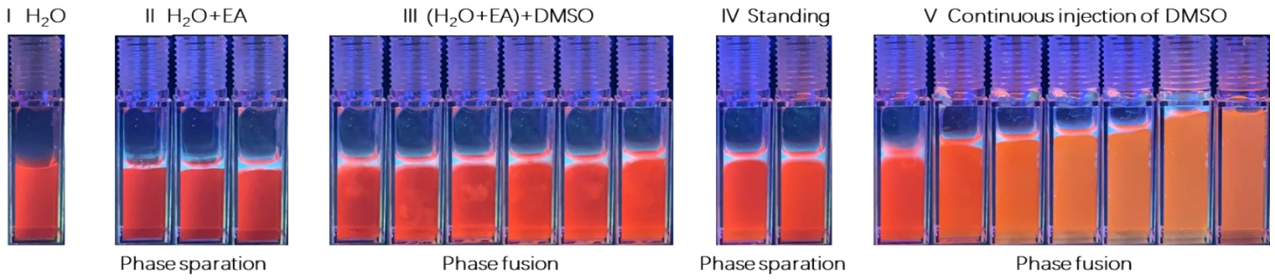

Fig. S24 Fluorescence photos of phase transition process visualized by PTZ, in which varying components of EA, DMSO, and water are mixed according to the established procedures.

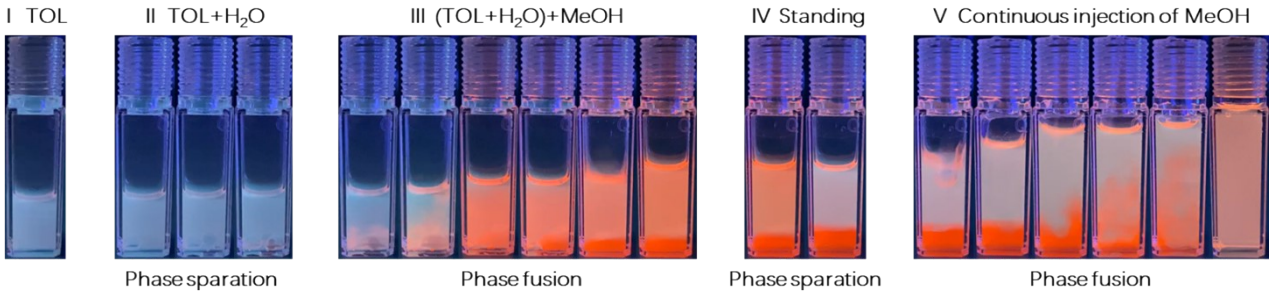

Fig. S25 Fluorescence photos of phase transition process visualized by PTZ, in which varying components of TOL, MeOH and water are mixed according to the established procedures.

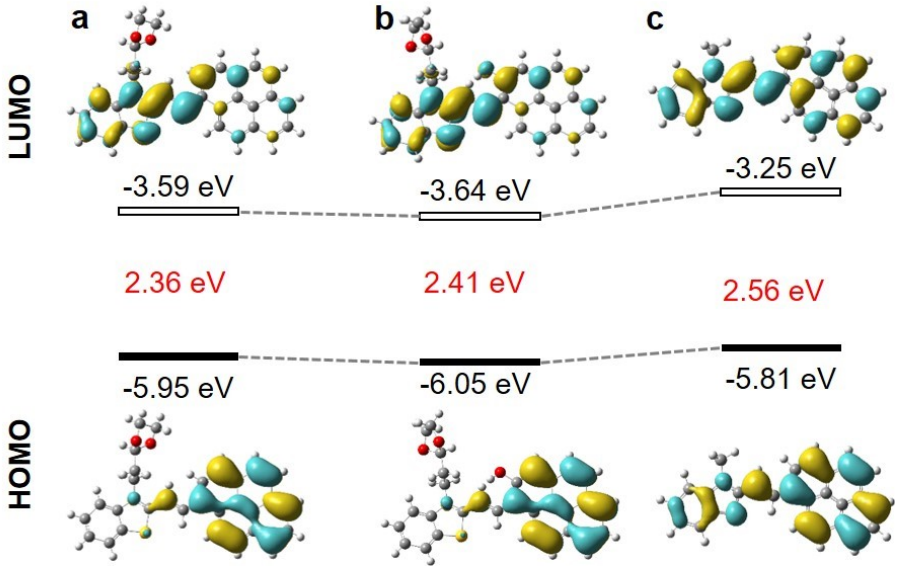

Fig. S26 The spatial electron distributions of HOMO and LUMO of PTZ (**a**), PTZ-OH (**b**), and PTZ-Me (**c**) at the B3LYP/6-31G (d, p) level in EA.

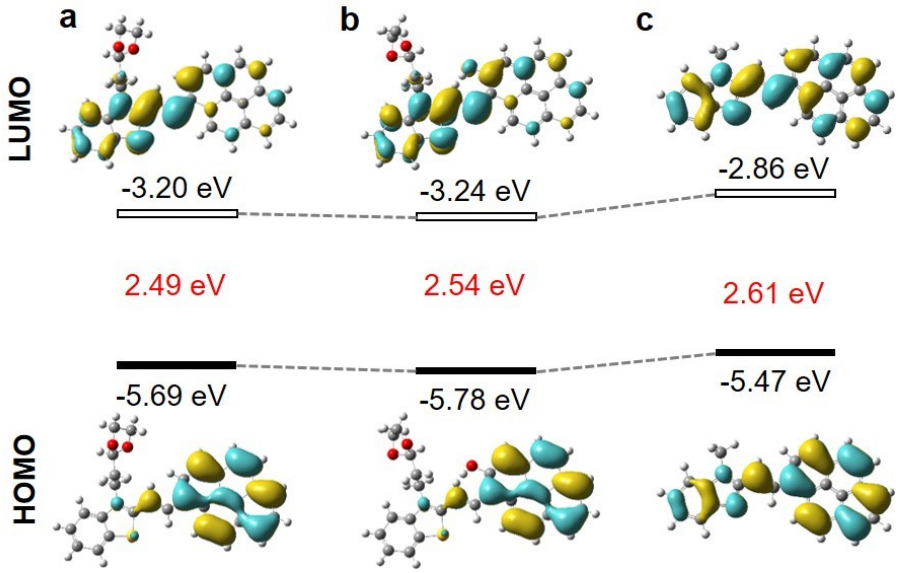

Fig. S27 The spatial electron distributions of HOMO and LUMO of PTZ (**a**), PTZ-OH (**b**), and PTZ-Me (**c**) at the B3LYP/6-31G (d, p) level in DMSO.

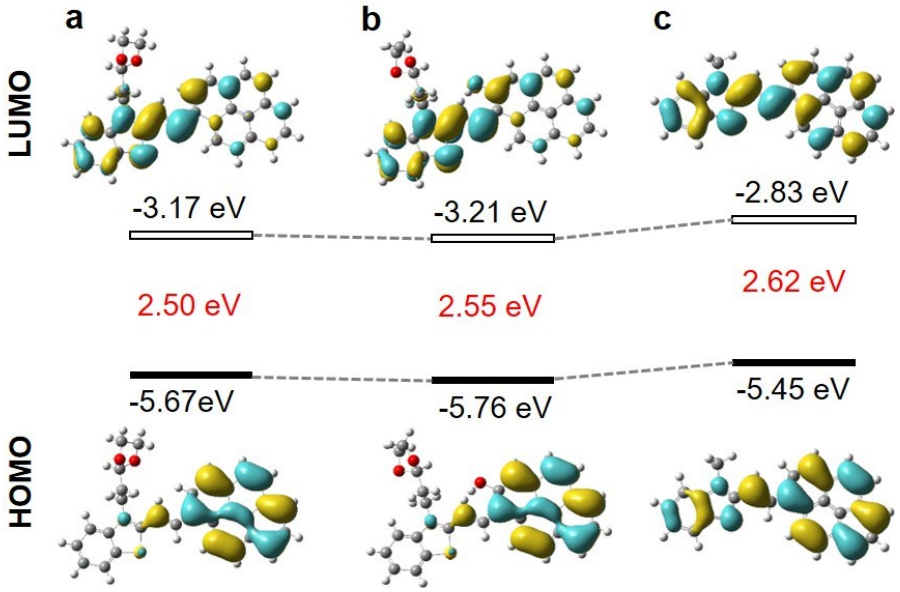

Fig. S28 The spatial electron distributions of HOMO and LUMO of PTZ (**a**), PTZ-OH (**b**), and PTZ-Me (**c**) at the B3LYP/6-31G (d, p) level in water.

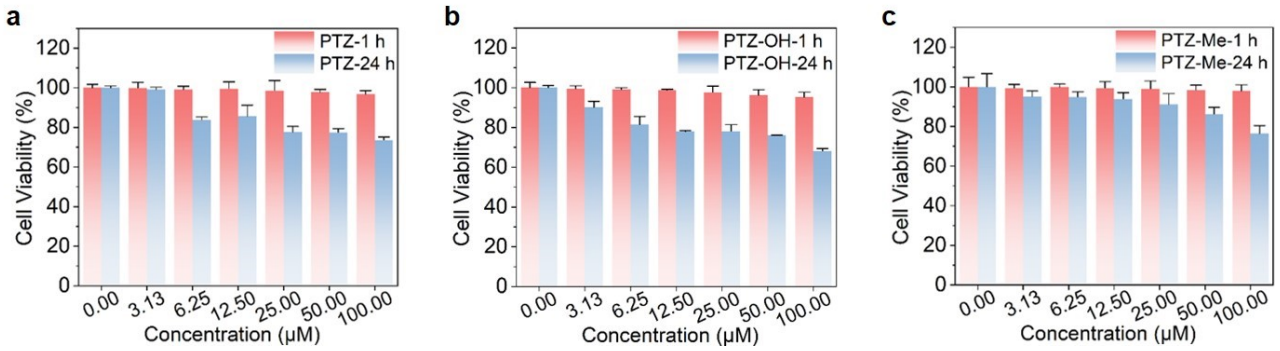

Fig. S29 MTT results of HeLa cells incubated with different concentrations of PTZ (**a**), PTZ-OH (**b**), and PTZ-Me (**c**) for 1 h and 24 h. The results indicated that the probe has good biocompatibility, and can be applied to cell imaging.

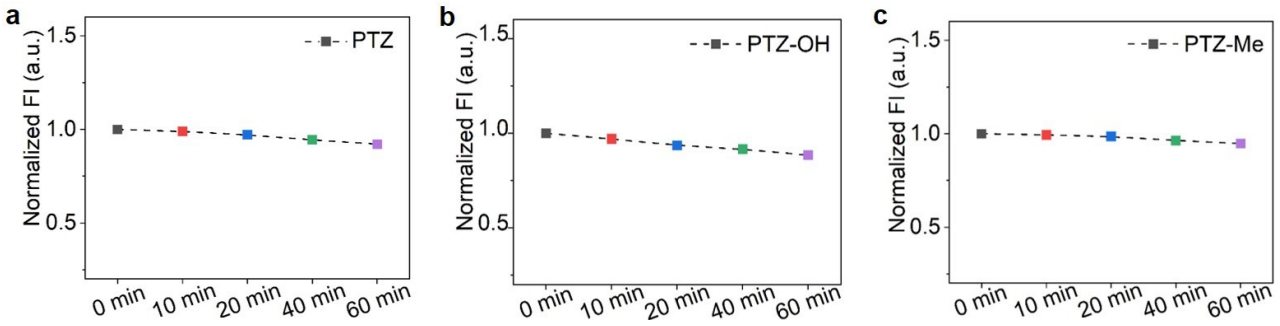

Fig. S30 The normalized fluorescence intensity of PTZ (**a**), PTZ-OH (**b**), and PTZ-Me (**c**) after exposure of UV lamp at 365 nm (12 W) for different time.

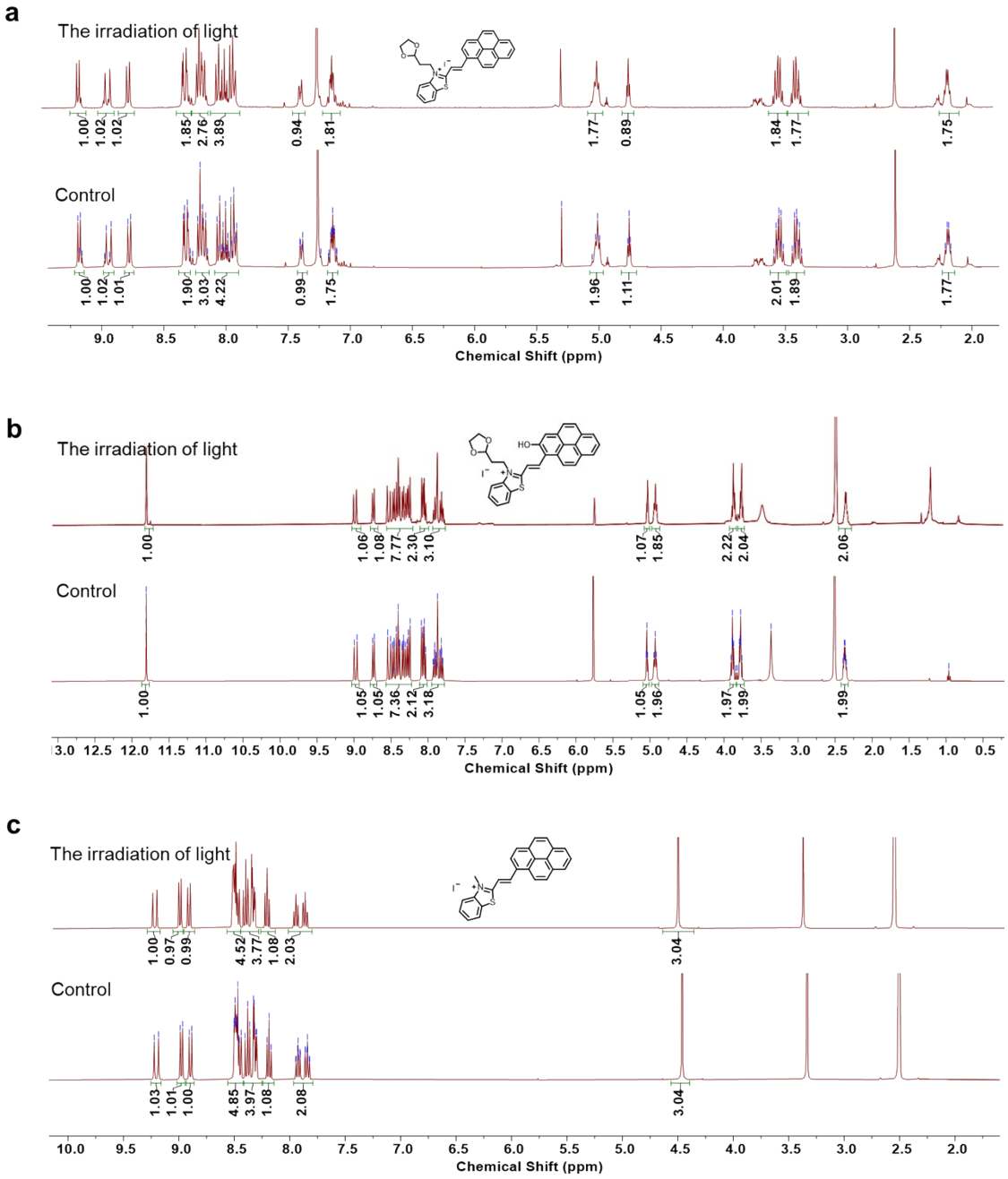

Fig. S31 ^{1}H NMR spectra of PTZ (**a**), PTZ-OH (**b**), and PTZ-Me (**c**) by irradiation for 2 h under UV lamp at 365 nm (12 W).

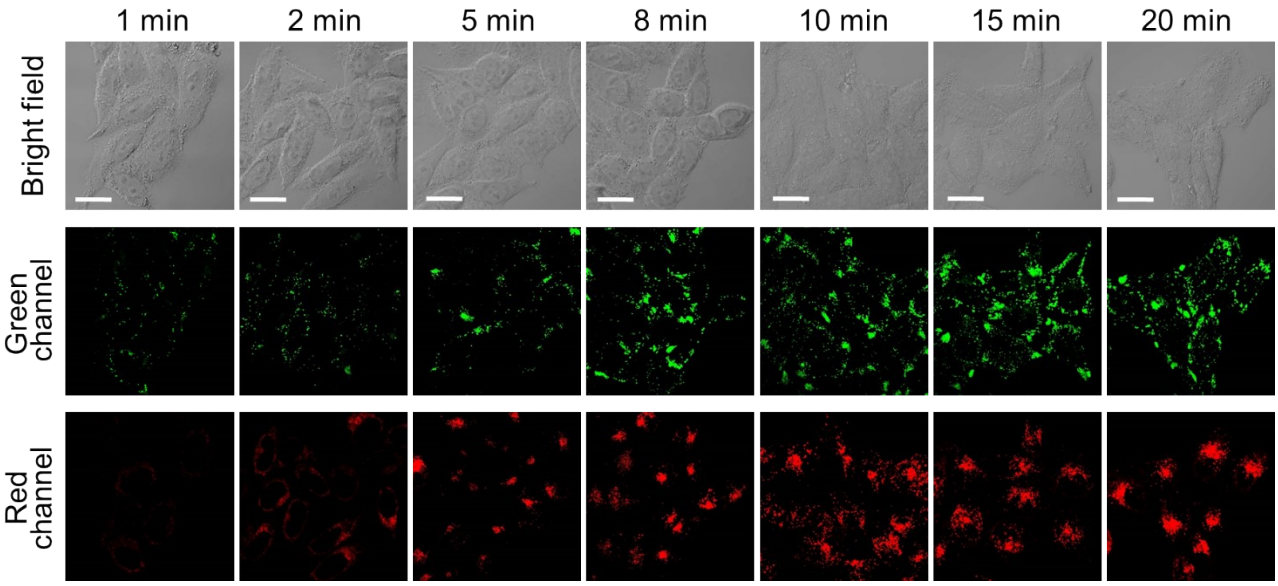

Fig. S32 CLSM images of HeLa cells incubated with PTZ (500 nM) for different incubation times. λ_{ex} = 405 nm; Green channel: λ_{em1} = 430-480 nm; Red channel: λ_{em2} = 570-630 nm; Scale bar: 20 μm.

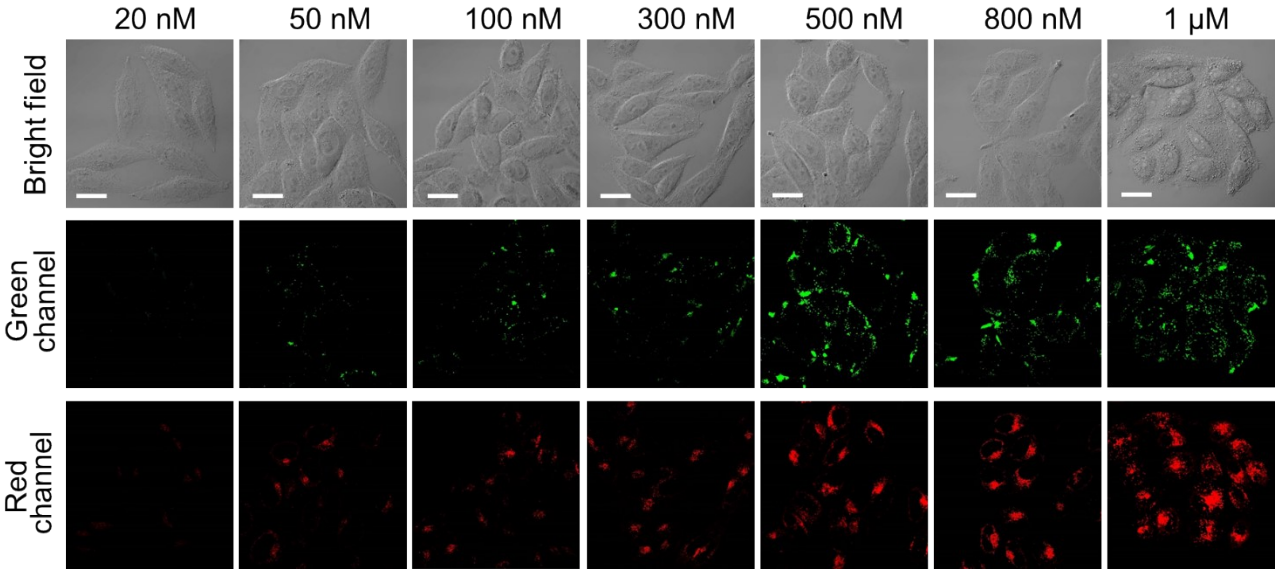

Fig. S33 CLSM images of HeLa cells stained with PTZ for 10 min at different incubation concentrations. λ_{ex} = 405 nm; Green channel: λ_{em1} = 430-480 nm; Red channel: λ_{em2} = 570-630 nm; Scale bar: 20 μm.

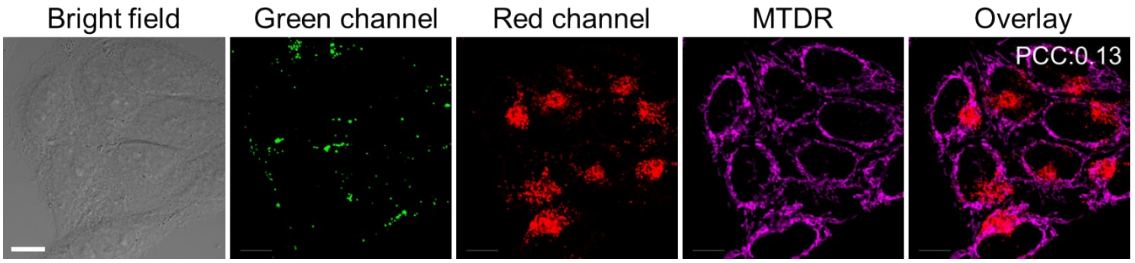

Fig. S34 Co-localization of PTZ (500 nM) with commercial mitochondria probe Mito Tracker™ Deep Red (MTDR, 200 nM). PCC: Pearson correlation coefficient. For PTZ, λ_{ex} = 405 nm, green channel: λ_{em} = 430-480 nm; red channel: λ_{em} = 570-630 nm. For MTDR, λ_{ex} = 633 nm, λ_{em} = 640-700 nm. Scale bar: 10 μm.

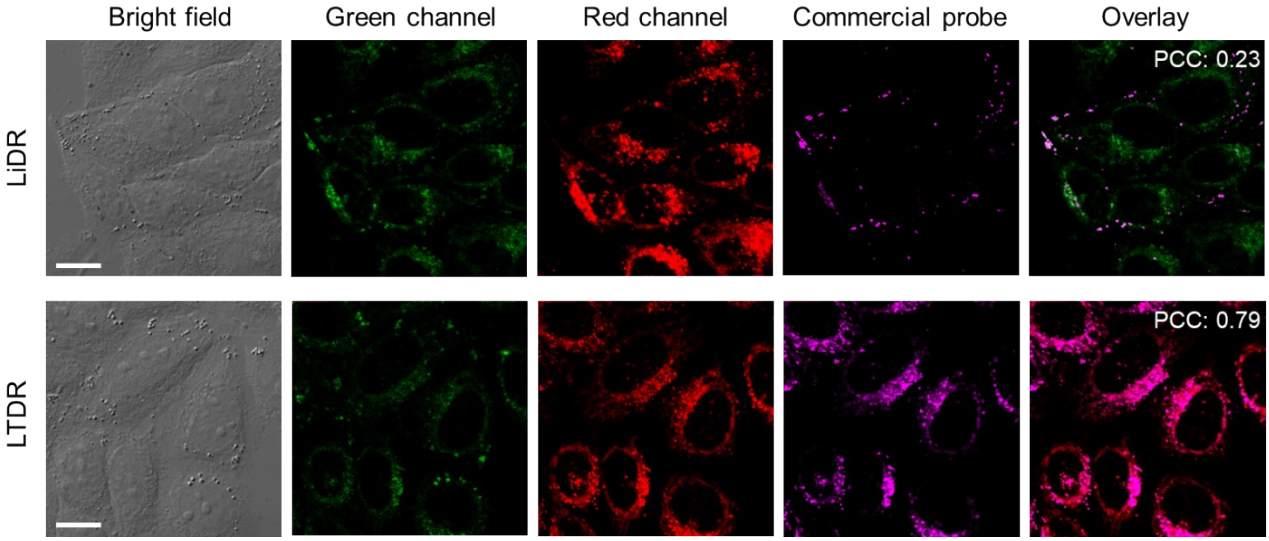

Fig. S35 Co-localization of PTZ-OH (1 μM) with commercial LDs probe LiDR (200 nM) or lysosome probe LTDR (200 nM). PCC: Pearson correlation coefficient. For PTZ-OH, λ_{ex} = 405 nm, green channel: λ_{em} = 430-480 nm; red channel: λ_{em} = 570-630 nm. For LiDR, λ_{ex} = 633 nm, λ_{em} = 645-705 nm. For LTDR, λ_{ex} = 633 nm, λ_{em} = 640-700 nm. Scale bar: 10 μm.

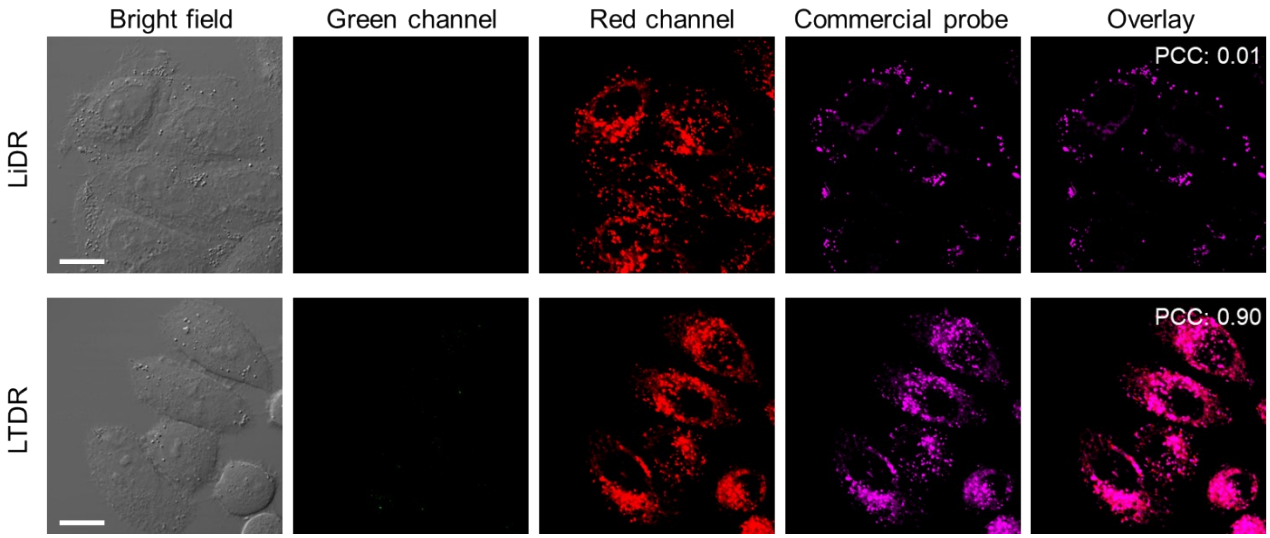

Fig. S36 Co-localization of PTZ-Me (1 μM) with commercial LDs probe LiDR (200 nM) or lysosome probe LTDR (200 nM). PCC: Pearson correlation coefficient. For PTZ-Me, λ_{ex} = 405 nm, green channel: λ_{em} = 430-480 nm; red channel: λ_{em} = 570-630 nm. For LiDR, λ_{ex} = 633 nm, λ_{em} = 645-705 nm. For LTDR, λ_{ex} = 633 nm, λ_{em} = 640-700 nm. Scale bar: 10 μm.

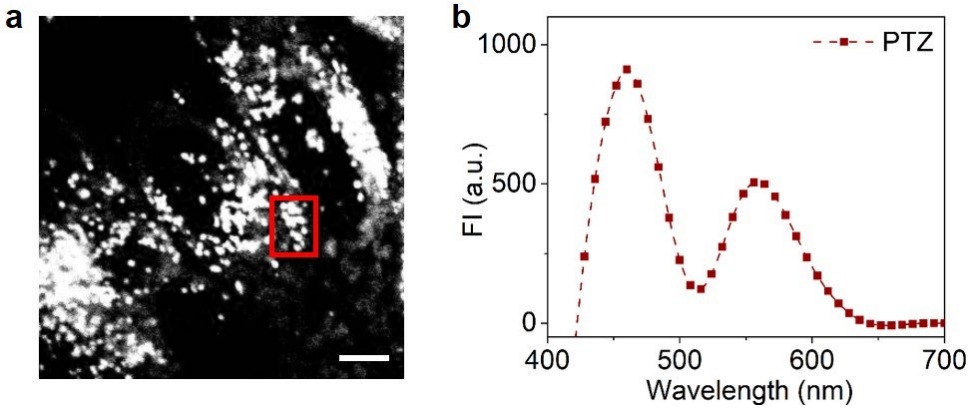

Fig. S37 Fluorescent grayscale image of PTZ (**a**) and its *in-situ* fluorescence spectrum (**b**) in living HeLa cells, Scale bar: 5 μm.

Table S1. Crystallographic parameters of PTZ.

Identification code	**PTZ**
Empirical formula	$C_{30}H_{24}NO_2SI$
Formula weight	635.53
Temperature/K	173.0
Crystal system	triclinic
Space group	P -1
Hall group	-P 1
a/Å	9.431(3)
b/Å	11.607(3)
c/Å	13.247(4)
α/°	87.189(9)
β/°	78.325(9)
γ/°	74.102(10)
Volume/Å^3	1365.7(6)
Z	2
ρ_{calc} g/cm^3	1.545
μ/mm^{-1}	10.200
F(000)	644.0
Crystal size/mm^3	0.08×0.06×0.01
Radiation	CuKα (λ=1.54178)
h,k,l_{max}	11,13,15
Nref	4781
T_{min},T_{max}	0.525，0.753
Theta(max)= 66.598	66.627
Data completeness	0.990
Final R indexes [I>=2σ (I)]	R_1=0.0295, wR_2=0.0783
Final R indexes [all data]	R_1= 0.0305, wR_2=0.0790

Table S2. The saturation solubility of PTZs in water, EA and MeOH.

S^a	S_{water}	S_{EA}	S_{MeOH}
PTZ	0.1509	0.1054	0.1878
PTZ-OH	0.0911	0.0268	0.2014
PTZ-Me	0.0837	0.0851	0.1210

Abbreviation: S^a = saturation solubility, the mass of solute dissolved when saturated in 100 g of solvent at room temperature.

Table S3. Photophysical properties of PTZs probes.

Compound	λ_{abs} (nm)	λ_{em} (nm)	Stokes shift (nm)	τ_{DMSO} (ns)	Φ_{EA} (%)	Φ_{DMSO} (%)	Φ_{water} (%)
PTZ	484	600	116	τ_1 =0.51(79.89%) τ_2 =1.96(20.11%)	1.05	10.78	1.96
PTZ-OH	482	592	110	τ_1 =3.63(80.05%) τ_2 =0.13(19.95%)	0.27	2.42	0.11
PTZ-Me	482	603	121	τ_1 =0.43(84.38%) τ_2 =0.76(15.62%)	0.88	8.30	0.99

Abbreviation: λ_{abs} = absorption maximum, acquired at a concentration of 10 μM; λ_{em} = emission maximum in DMSO. Φ_{EA} = absolute fluorescence quantum yield in EA; Φ_{DMSO} = absolute fluorescence quantum yield in DMSO; Φ_{Water} = absolute fluorescence quantum yield in Water. τ_{DMSO} = fluorescence lifetime in DMSO.

Table S4. Fluorescence lifetimes of PTZ for two emission peaks in DMSO and EA.

Compound	EA		DMSO	
	460 nm	600 nm	460 nm	600 nm
PTZ	0.72(67.23%)	0.31(88.38%)	0.51(79.89%)	0.49(94.29%)
	4.84(32.77%)	4.22(11.62%)	1.96(20.11%)	1.21(5.71%)

Table S5. The CIE1931 coordinates data of PTZ in EA/DMSO mixtures with different DMSO fractions (f_{DMSO}).

PTZ CIE1931	f_{DMSO} (vol%)									
	0% - 5%									
x	0.164	0.177	0.194	0.205	0.223	0.238	0.250	0.261	0.267	0.282
y	0.140	0.147	0.160	0.168	0.185	0.195	0.205	0.213	0.221	0.231
	6% - 10%									
x	0.289	0.297	0.297	0.301	0.307	0.305	0.307	0.312	0.315	0.322
y	0.242	0.248	0.247	0.252	0.258	0.257	0.260	0.268	0.271	0.273

Table S6. The CIE1931 coordinates data of PTZ-OH in EA/DMSO mixtures with different DMSO fractions (f_{DMSO}).

PTZ-OH CIE1931	f_{DMSO} (vol%)									
	0% - 5%									
x	0.174	0.174	0.191	0.198	0.198	0.200	0.124	0.205	0.206	0.215
y	0.081	0.083	0.109	0.153	0.160	0.178	0.229	0.245	0.261	0.332
	6% - 10%									
x	0.217	0.220	0.226	0.231	0.231	0.237	0.236	0.236	0.237	0.237
y	0.362	0.386	0.435	0.482	0.496	0.545	0.551	0.552	0.551	0.548

Table S7. The CIE1931 coordinates data of PTZ-Me in EA/DMSO mixtures with different DMSO fractions (f_{DMSO}).

PTZ-Me CIE1931	***f_{DMSO}*** (vol%)									
	0% - 5%									
x	0.450	0.450	0.449	0.454	0.468	0.476	0.497	0.506	0.512	0.526
y	0.458	0.455	0.464	0.463	0.463	0.461	0.455	0.452	0.450	0.445
	6% - 10%									
x	0.533	0.537	0.546	0.552	0.554	0.555	0.556	0.556	0.556	0.556
y	0.442	0.441	0.437	0.435	0.434	0.434	0.433	0.433	0.433	0.433

Table S8. Theoretical calculation for the dipole moments of PTZ in EA, DMSO, and water from B3LYP functional with 6-31+G (d) basis.

Solvent	X	Y	Z	μ (D)
EA	-11.99	-1.96	-1.19	11.23
DMSO	-12.00	-2.08	-1.35	12.25
Water	-12.06	-2.09	-1.36	12.32

Table S9. The hydrogen bonding interactions between PTZ and the three solvent.

Solvent	$E_{HB\text{-}1}$ (kcal/mol)	$E_{HB\text{-}2}$ (kcal/mol)
EA	-2.14	-2.45
DMSO	-3.31	-4.36
Water	-4.35	-7.92

5. References

1. Frisch, M. J., Trucks, G., Schlegel, H. B., Scuseria, G. E., Robb, M. A., Cheeseman, J. R., Scalmani, G., Barone, V., Mennucci, B. Petersson, G. A. 2009, *In Gaussian 09W, revision A*: 02,.

2. Eiring, P., McLaughlin, R., Matikonda, S. S., Han, Z., Grabenhorst, L., Helmerich, D. A., Meub, M., Beliu, G., Luciano, M., Bandi, V., Zijlstra, N.,Shi, Z. D., Tarasov, S. G., Swenson, R., Tinnefeld, P., Glembockyte, V., Cordes, T., Sauer, M. Schnermann, M. J. Targetable Conformationally Restricted Cyanines Enable Photon-Count-Limited Applications. *Angew. Chem. Int. Ed.* 2021, 60: 26685-26693.

3. Bi, S., Meng, F., Wu, D., Zhang, F., Synthesis of Vinylene-Linked Covalent Organic Frameworks by Monomer Self-Catalyzed Activation of Knoevenagel Condensation. *J. Am. Chem. Soc.* 2022, 144: 3653-3659.